CYBERNETICS AND PHYSICS, VOL. 15, NO. 1, 2026, 31–37

COMPUTER VISION ALGORITHMS FOR DERMOSCOPIC IMAGES

Elena D. Kotina
St. Petersburg State University
Russia
e.kotina@spbu.ru

Maria A. Nikoljukina
St. Petersburg State University
Russia
st107568@student.spbu.ru

Alexander V. Patrushev
Military Medical Academy
Russia
alexpat2@yandex.ru

Article history:
Received 12.02.2026, Accepted 19.06.2026

Abstract

The paper proposes algorithms for processing dermoscopic images: a preprocessing algorithm aimed at detecting noise on the image (hair structures and immersion gel bubbles) and subsequent restoration of color characteristics of the noisy skin areas; and a region of interest extraction algorithm that takes into account the specifics of dermoscopic images (possible low contrast in RGB space, characteristic of some types of skin lesions, preservation of hair fragments after preprocessing).

The proposed hair detection method is based on a combination of directional Gabor filters and Laplacian of Gaussian filters. This hybrid approach allows for the detection of both thick dark hair structures and thin light ones, demonstrating robustness to the properties of color, direction, and thickness of the detected objects. To minimize false positives at lesion boundaries, an additional geometric analysis of the mask using an elliptical test is proposed. This stage allows for an automatic decision on the need to apply the inpainting procedure, which helps preserve information about the texture of the skin lesion on weakly noisy images.

Key words

Dermoscopy, image processing, hair detection, segmentation, Gabor filters, Laplacian of Gaussian.

1 Introduction

Among oncological diseases, malignant skin neoplasms are the most common worldwide. The number of new cases of both malignant melanoma and nonmelanoma skin cancer (NMSC) is steadily increasing each year due to population aging and growth. Thus, incidence rates increased by 310% for squamous cell carcinoma, 161% for melanoma, and 77% for basal cell carcinoma between 1990 and 2017. It is predicted that this trend will continue in the coming decades. In this situation, timely and correct diagnosis is of key importance.

In general, the problem of skin neoplasm diagnostics remains unresolved for the healthcare systems of all countries. The key point is early diagnostics of malignant skin tumors, which significantly affects the patient's prognosis and financial costs of treatment. Even for such a deadly tumor as melanoma, diagnostics at stages I and II in most cases saves the patient's life, and further tactics involve only periodic control examinations and tests. In turn, late diagnostics at stages III and IV requires the appointment of expensive treatment (targeted drugs, immunotherapy) and complex surgical interventions.

Malignant tumors at an early stage often have minimal distinctive clinical and dermoscopic signs, sometimes an atypical clinical picture, for example, an amelanotic form of melanoma. In turn, benign neoplasms often "mask" as malignant ones. All this makes the diagnosis of skin tumors a difficult task.

Dermoscopy is a method of non-invasive skin examination that allows obtaining an enlarged image of its surface [Huang, 2020]. Using a dermatoscope provides the physician with an opportunity to more accurately assess the texture, shape, color of skin lesions and make a more accurate diagnosis. The immersion gel is a key physical element enabling dermoscopic imaging. The visualization of skin structures down to the papillary dermis occurs in a plane parallel to the skin surface due to the elimination of light reflection by the stratum corneum. This optical clearing effect is achieved because the refractive indices of the immersion fluid, the dermatoscope's contact plate glass, and the epidermis are closely matched. As a result, light rays pass through these media with negligible reflection at the boundaries, penetrate freely into the epidermis and dermis, and are reflected by structures located at these depths. The stratum corneum thus becomes effectively "transparent" to the observer, enabling examination of structures in the epidermis, at the dermoepidermal junction, and within the dermis [Agakishizadeh et al., 2022]. Dermoscopic images are high-resolution color images in RGB format with three channels.

Performing preliminary processing of dermoscopic images is a necessary stage in the diagnostics of skin neoplasms regardless of the classifier used further. The problem of image denoising is considered by many authors, and its solution involves approaches based on various mathematical frameworks [Thang et al., 2023; Mao et al., 2025]. For dermoscopic images, this stage is associated with a number of difficulties: high variability of noise (which includes hairs and, in the case of improper storage or application, air bubbles in the immersion gel layer), and the complexity of extracting features that allow separating noise and significant data (color characteristics of hairs and skin neoplasms are often indistinguishable, analysis of more complex characteristics – such as object shape – requires constructing banks of multi-directional filters [Abuzaghleh et al., 2015]).

A large number of works are devoted to preprocessing of these images, most often considering the task of hair removal on images. In the article [Lyakhov and Lyakhova, 2021], it was demonstrated that cleaning dermoscopic images from hairs improves classification quality.

Among global methods (applied to the entire image without dividing into sections), the work [Abuzaghleh et al., 2015] should be highlighted, where a set of 84 directional filters, representing differences between an isotropic and Gaussian filter, is used for the task of hair structure detection.

Often, for hair detection, transition from RGB to other color spaces (YIQ, LUV, etc.) is used [Zaqout, 2020; Pathan et al., 2018]. In particular, working with color spaces based on separating luminance and "chromaticity" components allows reducing the influence of illumination level on the algorithm's result, making these spaces (LUV, CIE LAB) more preferable for working with dermoscopic images. The use of morphological operations at the preprocessing stage of these images is also a widely used technique [Lyakhov and Lyakhova, 2021; Zaqout, 2020; Fiorese et al., 2011; Pathan et al., 2018].

Extracting the lesion area, or segmentation, is also considered in the literature as a necessary stage of computer-aided diagnostics [Smalyuk et al., 2024]. In [Pathan et al., 2018], two independent segmentation methods are proposed: one is based on extracting two principal components in LUV space, in the plane of which a 2D histogram is built. Then clustering is performed. The second proposed method is also applied in the aforementioned color space, but it is based on sequential use of color isotropic diffusion and the morphological "flooding" operation, allowing the extraction of isolines.

In recent years, deep learning has been increasingly applied in medical image segmentation tasks [Schmidt et al., 2023; Larochkin et al., 2025]; however, the specifics of dermoscopic images keep less resource-intensive algorithms competitive.

This article proposes a comprehensive approach to this task: the proposed algorithms are applied both to improve the images themselves and to extract the region of interest. For hair detection, a combination of Gabor filters and Laplacian of Gaussian filters is used, allowing the detection of other noise as well, including gel bubbles. For segmentation, a region growing algorithm with automatic determination of sensitivity threshold and starting points is proposed.

2 Image Preprocessing

This section proposes an algorithm for hair detection on dermoscopic images. Preprocessing includes constructing a mask based on the combined response of Gabor and Laplacian of Gaussian filters and making a decision on applying inpainting based on the analysis of geometric properties of the obtained mask to minimize information loss.

The proposed algorithm is a modification of the approach described in [Pathan et al., 2018]. The Pathan et al. approach avoids errors inherent to algorithms based on the assumption of a high degree of color difference between hairs and surrounding skin. This assumption leads to incorrect algorithm behavior in the case of benign lesions, when due to melanin distribution the skin lesion and hairs have low color variation, as well as in the case of light hairs. At the first stage, a bank of directional 2D Gabor filters is formed; parameter values for filter generation are selected according to [Pathan et al., 2018]:

$$G(x, y) = \exp\left[-\pi\left(\frac{x_q^2}{\sigma_x^2} + \frac{y_q^2}{\sigma_y^2}\right)\right] \cdot \cos(2\pi f x_q), \quad (1)$$

where:

$x_q = x\cos\theta_i + y\sin\theta_i$,
$y_q = -x\sin\theta_i + y\cos\theta_i$,
θ_i - filter orientation,
f - central frequency,
σ_x, σ_y - standard deviations.

Using a filter bank allows detecting hairs regardless of their direction. The feature of Gabor filters is their band-pass characteristics, determining the filters' ability to respond to structures of a certain range of spatial frequencies. This feature (for fixed generation parameter values) leads to high sensitivity to edge structures (hair contours), while the filter response for the part of the hair far from the boundary turns out to be quite weak.

In this regard, applying Gabor filters for thick hairs using fixed parameter values turns out to be ineffective (see Fig. 1).

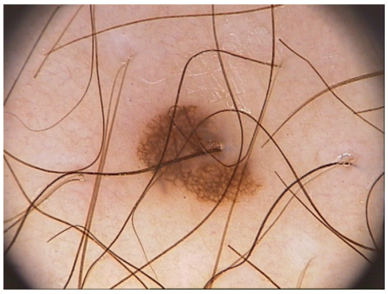

(a)

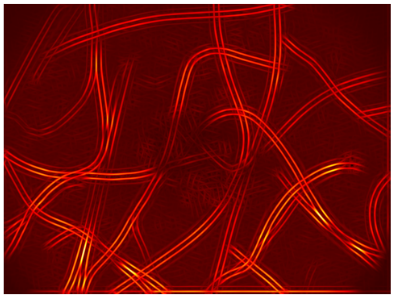

(b)

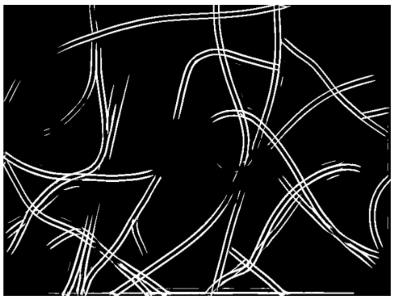

(c)

Figure 1. Applying Gabor filter highlights hair boundaries: (a) original image, (b) filter response, (c) binarized mask

To compensate for this limitation, as a second stage, it is proposed to also form a bank of Laplacian of Gaussian (LoG) filters.

$$\mathrm{LoG}(x, y) = -\left(1 - \frac{r^2}{2\sigma^2}\right) \cdot \exp\left(-\frac{r^2}{2\sigma^2}\right), \qquad (2)$$

where:

$r^2 = x^2 + y^2$,
σ - scale parameter.

It should be noted that the negative central peak of the LoG kernel shows high sensitivity to dark homogeneous areas, therefore in the case of thick light hairs, applying solely this set of filters will be ineffective. However, light hairs are generally thinner, which ensures detection of light hairs by Gabor filters. Thus, using a combination of Gabor and Laplacian of Gaussian filters allows achieving complete coverage of hair structures regardless of their direction, thickness and color characteristics (see Fig. 2).

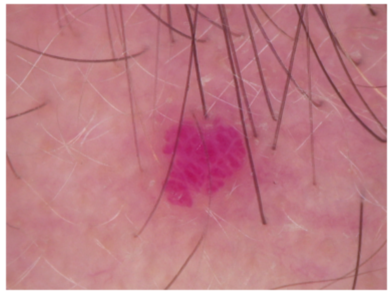

(a)

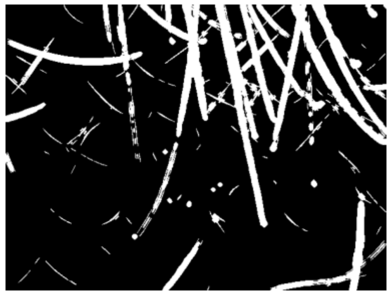

(b)

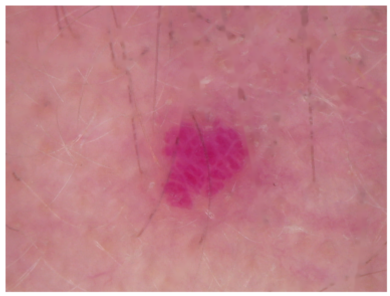

(c)

Figure 2. Using a combination of Gabor filters (removal of thin light hairs) and Laplacian of Gaussian filters (removal of thick dark hairs): (a) original image, (b) binarized mask, (c) preprocessed image

At the third stage, the combined output of Gabor and Laplacian of Gaussian filters is formed, which is defined as the maximum over all filters:

$$R_{\text{final}}(x, y) = \max\left\{ \max_{i=\overline{0,N}} R^{(i)}_{\text{gabor}}(x, y),\ \max_{i=\overline{0,N}} R^{(i)}_{\text{log}}(x, y) \right\}, \qquad (3)$$

where:

$R^{(i)}_{\text{gabor}} = G(x, y)_{\theta_i} \times L(x, y)$,
$R^{(i)}_{\text{log}} = \text{LoG(x, y)}_{\theta_i} \times L(x, y)$,
$L(x, y)$ - luminance channel in LAB color space,
$N = 15$ - number of orientations.

According to [Pathan et al., 2018], a GLCM matrix is then formed, and the binarization threshold is determined as the value that maximizes the total second-order entropy of local quadrants. This approach allows obtaining accurate hair masks in the case of homogeneous skin lesions and when there are hairs on the image. However, for images that do not require cleaning, determining the threshold based on maximizing the entropy of main GLCM matrix quadrants and subsequent inpainting leads to blurring the texture of the lesion itself (see Fig. 3). This result is explained by a significant decrease in threshold T in the case of "clean" images, so the relatively weak response of filters in areas of lesion inhomogeneity turns out to be large enough to overcome the threshold.

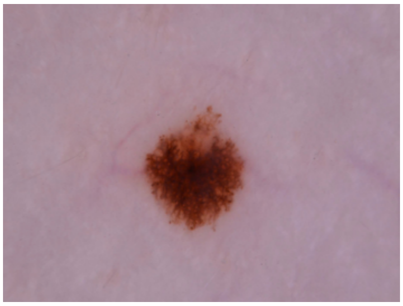

(a)

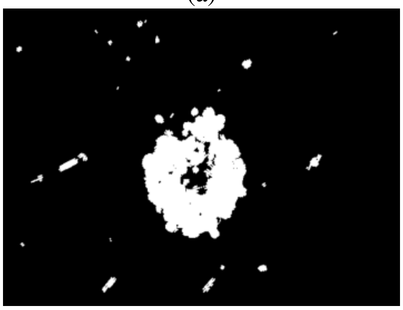

(b)

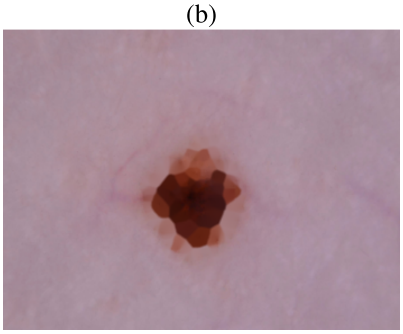

(c)

Figure 3. Loss of information about skin lesion texture as a result of applying filtering: (a) original image, (b) binarized mask, (c) image after applying filtering

To eliminate false positives on internal structures, additional filtering based on geometric features of the obtained mask was performed. As mentioned above, in the case when the image is not noisy with hairs, the binary mask includes pixels corresponding to the inner part of the skin lesion, which leads to a characteristic mask appearance with a compact area of high density (see Fig. 3b).

To detect such cases, the following algorithm is proposed: the main contour (the largest area of pixels with value True) is found on the mask, which is approximated by an ellipse. Then the properties of the obtained ellipse are evaluated: fill density and axis ratio, ellipse area. Fill density and axis ratio allow determining masks that have detected hairs: if the density value $\rho < \rho_{threshold}$ or the axis ratio $ratio > ratio_{threshold}$, the mask has detected hairs, since they have an elongated shape. The ellipse area must be above the threshold $s_{threshold}$, which avoids considering masks that have detected only bubbles from the gel applied during dermoscopy, or other small objects. Visualization of the algorithm's operation is presented in Fig. 4.

Based on the result of the elliptical test, a decision is made on applying inpainting. If the mask does not satisfy at least one of the conditions described above, inpainting is not applied. Thus, the elliptical test allows preserving information about the lesion texture when the image turns out to be weakly noisy.

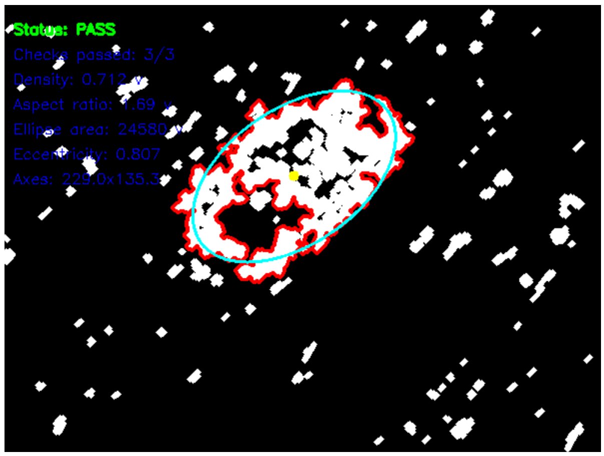

(a)

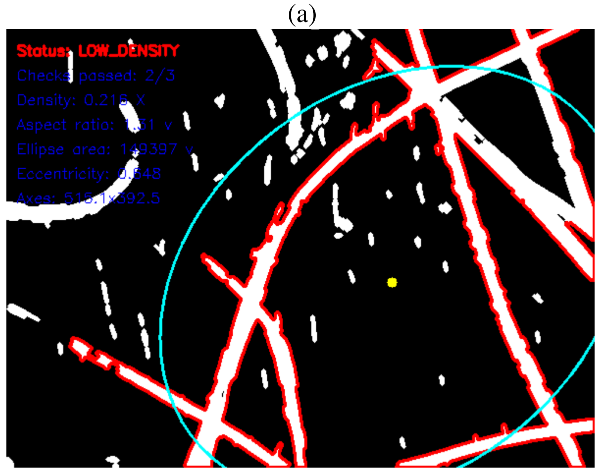

(b)

Figure 4. Visualization of the elliptical test operation: (a) test result positive, preprocessing skipped, (b) test result negative, processing applied

3 Segmentation

For extracting the region of interest, region growing from seed points is applied. The selection of the sensitivity value of the region growing algorithm (a parameter determining how similar pixel values should be to unite them into one region) is performed in two stages: enumeration with calculation of the contour length corresponding to each parameter value, and automatic selection based on the dynamics of contour length change. After extracting the region of interest, postprocessing of the obtained binary mask is performed.

The algorithm for selecting starting growth points should be considered separately. Importantly, the standard conversion from an RGB image to a single-channel GRAY format, which is performed using the formula

$$Gray = 0.2989 * R + 0.5870 * G + 0.1140 * B, \quad (4)$$

or to the L channel of the CIE LAB color space, which allows working with object intensity on the image [Ly et al., 2020], and choosing the darkest pixel as the starting point is not universal (see Fig. 5). As shown in Figure 5, pixel intensity does not always allow determining the region of interest. Moreover, in the case when after the preprocessing stage hair fragments remain on the image, the starting growth point chosen as the darkest pixel can lead to growing a contour for a hair fragment, not for the skin lesion.

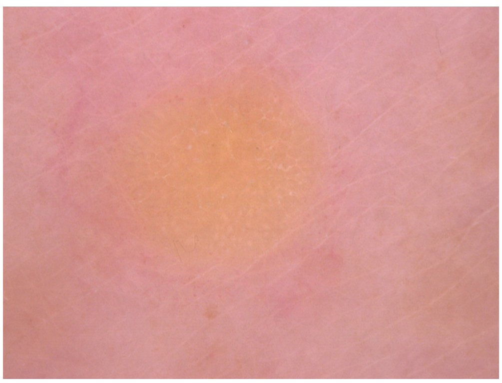

(a)

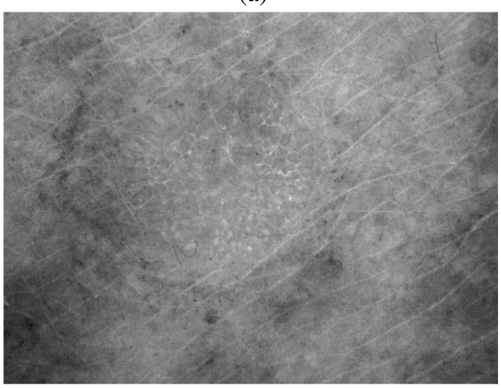

(b)

Figure 5. Case of indistinguishability of pixel intensities belonging to the lesion and pixels belonging to skin: (a) original image, (b) L-component of the image in CIE LAB space (pixel brightness)

To overcome the described limitations, the following approach with multiple selection of starting points is proposed: the first step is constructing intensity profiles: horizontal and vertical profiles passing through the center of the image are built (it is assumed that in most cases the lesion intersects at least one of the axes). The second step is approximating the obtained histograms with a fourth-degree polynomial. The third step is determining starting points. Since the inflection points of the approximating polynomial allow approximately separating the region of interest from the background, the intensity profile is divided into segments by inflection points. Then, on each segment, a point of local maximum or minimum (depending on the polynomial behavior on this segment) of the original histogram is selected. The set of points selected in this way represents the set of starting points for region growth. This approach avoids incorrect extraction of the region of interest due to preserved noise after preprocessing. The fourth step is contour growing. To determine the threshold of permissible pixel dissimilarity (parameter of the used BFS growing algorithm for region growing), an adaptive approach is used. For each growth point, iterative region growing is performed with sequential increase of the threshold from 0.05 to 0.9.

Upon completion of the iterative process, the dynamics of growth of the contour length of the segmented region are analyzed. The critical threshold is considered to be the point preceding the last sharp increase in contour length relative to the length at the previous iteration, which corresponds to the transition from segmentation of the lesion itself to capturing the surrounding skin. The increase in contour length is chosen as a criterion because when the grown region goes beyond the lesion, its area increases significantly (usually the background after preprocessing becomes highly homogeneous); moreover, in the case when the skin around the lesion has pronounced features (case of non-uniform background) - vascular network, pigmentation, the boundary of the region will become more complex (going around these features), which will also lead to a jump in contour length. The iteration before the last jump corresponds to the optimal threshold value. The last jump is considered because for the first few parameter values jumps will be observed in relation to contour lengths at the current and previous iterations (due to small length values).

If the mask built by the described method includes more than two corner pixels or the obtained optimal threshold value is below 0.4, an additional check is performed to solve the problem of low intensity variation described above: as the monochannel for building histograms, the b-component of the CIE LAB space with subsequent inversion is chosen. The choice of this component is motivated by the fact that the problem of weak distinguishability of the region of interest and background in grayscale and L channels is characteristic for lesions having light-yellow shades, easily separable in the b-channel from more bluish skin (see Fig. 6).

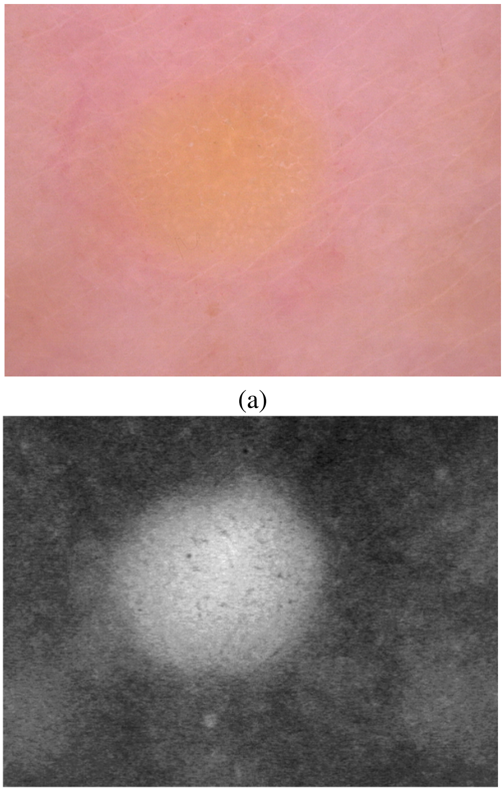

(a)

(b)

Figure 6. Using the b-component in case of indistinguishability of pixel intensities belonging to the lesion and pixels belonging to skin: (a) original image, (b) b-component of the image in CIE LAB space

It should be noted that despite the initial assumption that the lesion area intersects at least one of the image's middle lines, region growing allows obtaining correct masks in the general case as well. Choosing growth points from each segment between inflection points allows growing contours from background pixels, so in the case when none of the selected points belongs to the skin lesion, a mask that has extracted only pixels not related to the region of interest will be obtained. Thus, applying logical negation will allow switching to a correct mask. Figure 7 shows an example of the result of the mask construction algorithm.

After constructing the mask, postprocessing is performed: in the case when after preprocessing hairs intersecting the region of interest remain on the image, they will be represented on the mask as elongated protruding areas. For thin hairs, the morphological opening operation is applied, but in the case of thick hairs the erosion kernel must have significantly larger sizes, which can lead to loss of information about the skin lesion boundary when applying this operation. Therefore, a geometric algorithm based on analyzing distances from the mask's center of mass to points on its contour is used.

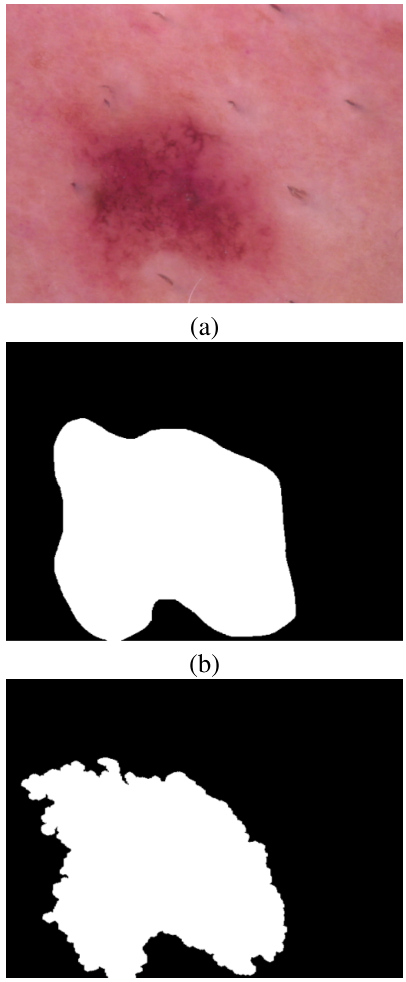

(a)

(b)

(c)

Figure 7. Comparison of algorithm application results with ground truth mask: (a) original image, (b) ground truth mask, (c) mask built by the algorithm

This analysis allows identifying elongated structures characteristic of hair shafts. First, the necessity of applying processing is determined by comparing the areas of the mask and its convex hull – if the value is below the threshold, processing is skipped. Then, for each contour point, the Euclidean distance to the center of mass of the mask is calculated, and based on the obtained distribution, the mean value and standard deviation are calculated. Contour points whose distance to the center of mass exceeds $\mu + \alpha\sigma$ (α – adjustable sensitivity threshold) are identified as potential hairs. Then outliers are grouped by adjacent angular sectors, which allows removing entire hair structures, and in the specified angular ranges all pixels located farther than the average radius from the center of mass are removed. The result of applying the described postprocessing method is shown in Fig. 8.

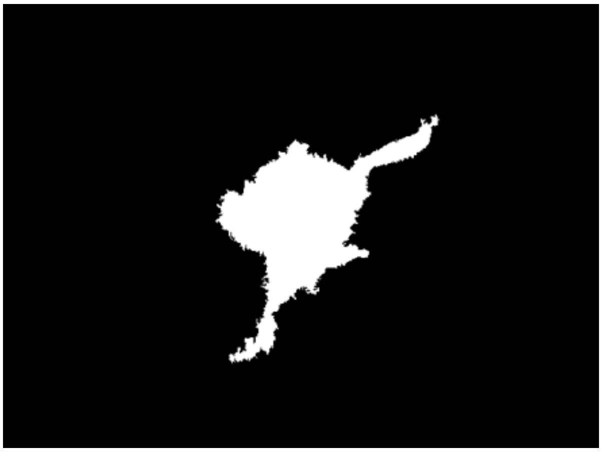

(a)

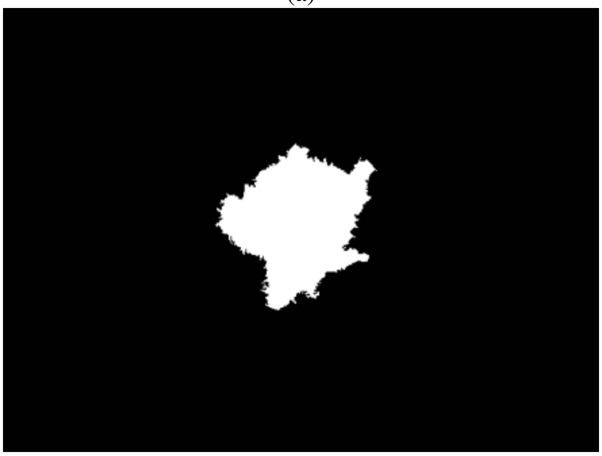

(b)

Figure 8. Result of applying the postprocessing algorithm to the segmented region: (a) original mask, (b) mask after postprocessing

4 Conclusion

Within the work, a solution to two interrelated tasks of automated analysis of dermoscopic images is proposed: preprocessing and region of interest extraction. A hybrid method combining analysis of textural features (Gabor filters) and detection of dark homogeneous areas (Laplacian of Gaussian filters) is developed. To minimize false positives, a criterion analyzing geometric characteristics of the formed mask is introduced. This approach prevents loss of information about the neoplasm texture. Additionally, an adaptive algorithm based on region growing is proposed, automatically determining a set of starting points by analyzing intensity profiles, as well as optimizing the sensitivity parameter by tracking the dynamics of change in the contour length of the segmented region.

References

Abuzaghleh, O., Barkana, B. D., and Faezipour, M. (2015). Noninvasive real-time automated skin lesion analysis system for melanoma early detection and prevention. *IEEE Journal of Translational Engineering in Health and Medicine*, **3**, pp. 1–12.

Agakishizadeh, N. E., Gafton, I. G., Zinoviev, G. V., Gafton, G. I., Chuglova, D. A., Ebert, M. A., Sinyachkin, M. S., Rogachev, M. V., Krzhivitskiy, P. I., Borodulin, A. V., Baykalova, O. I., Voropaeva, M. V., and Andrievskikh, E. A. (2022). *Modern Methods of Non-Invasive Diagnostics of Melanocytic Skin Neoplasms*. N.N. Petrov National Medical Research Center of Oncology, St. Petersburg.

Fiorese, M., Peserico, E., and Silletti, A. (2011). Virtualshave: automated hair removal from digital dermatoscopic images. In *Proceedings of the Annual International Conference of the IEEE Engineering in Medicine and Biology Society*, pp. 5145–5148. PMID: 22255497.

Huang, S. (2020). Dermoscopy: The essentials. *Skinmed*, **18** (3), pp. 192. PMID: 32790621.

Larochkin, P., Kotina, E., Girdyuk, D., and Ostroumov, E. (2025). Deep learning methods for right ventricle segmentation in radionuclide imaging. *Cybernetics and Physics*, **14** (1), pp. 62–66.

Ly, B. C. K., Dyer, E. B., Feig, J. L., Chien, A. L., and Bino, S. D. (2020). Research techniques made simple: Cutaneous colorimetry: A reliable technique for objective skin color measurement. *Journal of Investigative Dermatology*, **140**, pp. 3–12.

Lyakhov, P. A. and Lyakhova, U. A. (2021). Neural network classification system for pigmented skin neoplasms with preliminary hair removal in photographs. *Computer Optics*, **45** (5), pp. 728–735.

Mao, J., Sun, L., Chen, J., and Yu, S. (2025). Overview of research on digital image denoising methods. *Sensors*, **25** (8), pp. 2615.

Pathan, S., Prabhu, K., and Siddalingaswamy, P. C. (2018). Hair detection and lesion segmentation in dermoscopic images using domain knowledge. *Medical & Biological Engineering & Computing*, **56**, pp. 1–13.

Schmidt, I., Kotina, E., and Buev, P. (2023). Deep learning muscle segmentation model for ct images in dicom format. *Cybernetics and Physics*, **12** (3), pp. 201–206.

Smalyuk, A. F., Dzeshka, M. S., and Kupchykava, I. D. (2024). Segmentation of dermatoscopic images of skin lesions. comparison of methods. *System Analysis and Applied Information Science*, (1), pp. 50–58. In Russian.

Thang, P. C., Tran, T., Dang, H., and Mai, V. (2023). A non–convex total generalized variation model for image denoising. *Cybernetics and Physics*, **12** (1), pp. 70–81.

Zaqout, I. (2020). *An Efficient Block-Based Algorithm for Hair Removal in Dermoscopic Images*. IntechOpen.